Development 138, 1173-1181 (2011) doi:10.1242/dev.054049

Aplexone targets the HMG-CoA reductase pathway and differentially regulates arteriovenous angiogenesis

Jayoung Choi[1,*], Kevin Mouillesseaux[1,*], Zhiming Wang[2], Hannah D. G. Fiji[2], Sape S. Kinderman[2], Georg W. Otto[3,†], Robert Geisler[3,‡], Ohyun Kwon[2,4,5] and Jau-Nian Chen[1,4,5,6,§]

SUMMARY

Arterial and venous endothelial cells exhibit distinct molecular characteristics at early developmental stages. These lineage-specific molecular programs are instructive to the development of distinct vascular architectures and physiological conditions of arteries and veins, but their roles in angiogenesis remain unexplored. Here, we show that the caudal vein plexus in zebrafish forms by endothelial cell sprouting, migration and anastomosis, providing a venous-specific angiogenesis model. Using this model, we have identified a novel compound, aplexone, which effectively suppresses venous, but not arterial, angiogenesis. Multiple lines of evidence indicate that aplexone differentially regulates arteriovenous angiogenesis by targeting the HMG-CoA reductase (HMGCR) pathway. Treatment with aplexone affects the transcription of enzymes in the HMGCR pathway and reduces cellular cholesterol levels. Injecting mevalonate, a metabolic product of HMGCR, reverses the inhibitory effect of aplexone on venous angiogenesis. In addition, aplexone treatment inhibits protein prenylation and blocking the activity of geranylgeranyl transferase induces a venous angiogenesis phenotype resembling that observed in aplexone-treated embryos. Furthermore, endothelial cells of venous origin have higher levels of proteins requiring geranylgeranylation than arterial endothelial cells and inhibiting the activity of Rac or Rho kinase effectively reduces the migration of venous, but not arterial, endothelial cells. Taken together, our findings indicate that angiogenesis is differentially regulated by the HMGCR pathway via an arteriovenous-dependent requirement for protein prenylation in zebrafish and human endothelial cells.

KEY WORDS: HMGCR, Angiogenesis, Artery, Statin, Vein, Zebrafish

INTRODUCTION

Blood vessels are diverse in size, structure and function to suit the needs of their local tissue environment. Endothelial cells (ECs), the inner lining of the blood and lymphatic vessels, have instructive roles in specifying vascular architecture and physiology. Prior to the initiation of blood circulation, ECs have already assumed specific molecular characteristics based on their arterial or venous identities. For example, in zebrafish embryos, ECs of the dorsal aorta (DA) activate a transcriptional program involving expression of *notch* and *ephrinB2a* upon stimulation by VEGF, whereas ECs of the posterior cardinal vein (PCV) express a distinct set of genes such as *ephB4* and *flt4* (Lawson et al., 2001; Zhong et al., 2001; Lawson et al., 2002). Similarly, in mouse embryos, capillaries of arterial origin express ephrin B2 and those of venous origin express *Ephb4* (Wang et al., 1998). Disrupting this arteriovenous lineage-specific expression pattern blocks circulation, highlighting the essential role for arteriovenous identity in establishing blood circulation (Gerety et al., 1999; Gerety and Anderson, 2002).

In addition to the diversity in their transcriptional profiles, ECs exhibit different cellular behaviors according to their arteriovenous origins. In zebrafish, angioblasts migrate from their lateral position to the midline in two waves to form the vascular cord. It has been hypothesized that angioblasts destined to form the DA migrate first, whereas the angioblasts destined to form the PCV migrate at a later stage (Torres-Vazquez et al., 2003; Jin et al., 2005; Williams et al., 2010). A pathway involving signaling molecules such as VEGF, Notch, PI3K and Eph/ephrin then directs a dorsal migration of ECs to form DA and a ventral migration to form PCV (Herbert et al., 2009). The diversity in lineage-dependent cellular behavior is further evident in the differential timing of angiogenesis during the formation of the dorsoventrally positioned intersegmental vessels (ISVs) in the trunk. Two waves of ISV sprouting were noted in zebrafish depending on the origin of ECs (Isogai et al., 2003; Hogan et al., 2009; Ellertsdottir et al., 2010). The first wave occurs at around 20 hours post fertilization (hpf) when ECs of the DA migrate dorsally in response to signals, including VEGF and Notch to form the primary, aorta-derived vascular network. The second wave occurs about 16 hours later (36 hpf) when a new set of vascular sprouts emerges exclusively from the PCV. Some of these secondary sprouts connect with the primary ISVs, linking the posterior cardinal vein to the primary vascular network (Isogai et al., 2003; Hogan et al., 2009; Ellertsdottir et al., 2010). The distinct timings of the arterial-derived primary sprouts and the venous-derived secondary sprouts indicate that arterial and venous angiogenesis are differentially regulated during development.

[1]Department of Molecular, Cell and Developmental Biology, University of California, Los Angeles, CA 90095, USA. [2]Department of Chemistry and Biochemistry, University of California, 607 Charles E. Young Drive East, Box 951569, Los Angeles, CA 90095-1569, USA. [3]Abteilung III-Genetik, Max-Planck-Institut für Entwicklungsbiologie, Tübingen 72076, Germany. [4]Molecular Biology Institute, University of California, Paul D. Boyer Hall, 611 Charles E. Young Drive East, Los Angeles, CA 90095-1570, USA. [5]Jonsson Comprehensive Cancer Center, University of California, 8-684 Factor Building, Box 951781, Los Angeles, CA 90095-1781, USA. [6]Cardiovascular Research Laboratory, University of California, 675 Charles E. Young Drive South, MRL 3645, Los Angeles, CA 90095, USA.

*These authors contributed equally to this work
[†]Present address: Bioinformatics Core, The Wellcome Trust Centre for Human Genetics, Roosevelt Drive, Oxford OX3 7BN, UK
[‡]Present address: Institute of Toxicology and Genetics, Karlsruhe Institute of Technology, Hermann-von-Helmholtz-Platz 1, 76344 Eggenstein-Leopoldshafen, Germany
[§]Author for correspondence (chenjn@mcdb.ucla.edu)

Accepted 21 December 2010

How the distinct molecular identities of arteries and veins influence lineage-specific angiogenesis is currently not known. The optical clarity and rapid development of zebrafish embryos, along with the fact that they are fertilized externally, offer an excellent opportunity to conduct in vivo screens for compounds that modulate biological processes of interest (Zon and Peterson, 2005; Walsh and Chang, 2006). Traditionally, ISV formation has served as a model for angiogenesis in zebrafish. Here, we show that ECs of the caudal vein also undergo active angiogenesis, providing an additional model for venous angiogenesis. We screened a collection of small molecules for compounds that preferentially suppress angiogenesis by endothelial cells of either arterial or venous origin, using caudal vein morphogenesis and ISV formation as indicators. In this screen, we identified a novel compound, aplexone, that can effectively block angiogenesis from the vein, but has limited impact on arterial angiogenesis. We offer several lines of evidence demonstrating that aplexone targets the HMG-CoA reductase pathway, disrupts protein geranylgeranylation and effectively inhibits venous EC migration both in zebrafish embryos and cultured human ECs. In addition, we find that venous ECs have higher levels of proteins requiring geranylgeranylation than arterial ECs, and their migration is more sensitive to changes in protein prenylation. Taken together, our findings indicate that angiogenesis is differentially regulated based on the arteriovenous origin of ECs and that the HMGCR biochemical pathway has a crucial role in influencing the angiogenic migration.

MATERIALS AND METHODS

Zebrafish husbandry

The *Tg(kdrl:GFP)*^{la116} and *Tg(myl7:GFP)* transgenic lines and *smo*^{hi1640} were used for this study (Chen et al., 2001; Huang et al., 2003; Choi et al., 2007). Adult fish and embryos were maintained as previously described (Westerfield, 2000).

Imaging

Images of GFP expression in *Tg(kdrl:GFP)* embryos were acquired using a Zeiss SV-11 epifluorescence microscope. Confocal images were acquired using a Carl Zeiss Laser Scanning Systems LSM510 equipped with 20× air, 20× water or 40× water immersion objectives. For single time point confocal images, embryos were anesthetized with 0.01% tricaine and embedded in 1% agarose. When capturing time-lapse confocal movies, embryos were mounted in 3.5% methylcellulose (Sigma-Aldrich) and imaged for 5 hours on a heated stage at 28.5°C. The images obtained were analyzed using the Zeiss LSM Image Brower version4 and Image J.

Chemical screen and aplexone treatment

A synthetic chemical library containing 168 compounds (Castellano et al., 2007) and 300 chemicals from Biomol International, consisting of 72 ion channel inhibitors (Cat No. 2805), 84 kinase/phosphatase inhibitors (Cat No. 2831), 84 orphan ligands (Cat No. 2825) and 60 endocannabinoids (Cat No. 2801) were screened. The synthetic small molecules were prepared through nucleophilic phosphine catalysis of allenoates (Zhu et al., 2003). Four *Tg(kdrl:GFP)* embryos were placed into each well of 96-well plates containing a 10 μM solution of each chemical compound dissolved in embryo buffer with 0.1% DMSO. The embryos were raised at 28.5°C and examined for defects in blood vessel development at 1 and 2 days after treatment. Standard parameters such as numbers of somites and head to body angle were used to determine the stages of zebrafish embryos (Kimmel et al., 1995).

Aplexone treatment described in this study was carried out at a concentration of 10 μM, starting at 10 hpf unless otherwise specified.

Microarray and quantitative RT-PCR

Embryos at the five-somite stage were treated with 0.4% DMSO (control) or 10 μM of aplexone in 0.4% DMSO, and total RNA was isolated using the RNAeasy micro kit (Qiagen) at 30 hpf. Microarray analysis was performed in triplicate using the Affymetrix Zebrafish GeneChip, representing 15,617 genes. Synthesis and labeling of antisense RNA was performed as recommended by the array manufacturer using kits from Invitrogen for double-stranded cDNA synthesis, Enzo Life Sciences for transcription and labeling of antisense RNA, and Affymetrix for probe purification and hybridization controls. Microarray hybridization data were analyzed using scripts written in the statistical programming language R (R Development Core Team, 2010). Differentially expressed genes (DEGs) were identified using a linear model and multiple testing correction from the *limma* package (Smyth, 2004). The expression values were obtained using the robust multi array algorithm (Irizarry et al., 2003).

Quantitative RT-PCR was performed as follows. First-strand cDNA was synthesized using the SuperScript first-strand synthesis system for RT-PCR (Invitrogen) and relative expression levels of genes were determined using iQ SYBR Green Supermix and an iCycler (Bio-Rad Laboratories). GAPDH was used for normalization. Sequences of primers used in this study are provided in Table S2 in the supplementary material.

All expression data were deposited to the European Bioinformatics Institute's ArrayExpress (http://www.ebi.ac.uk/arrayexpress/) database with accession number E-MTAB-494.

Cholesterol assay

The yolk was removed from embryos by vortexing in calcium-free Ringer's solution with 1 mM EDTA at 4°C. The embryos were then pelleted and washed with fresh calcium-free Ringer's solution five times before being resuspended in cholesterol assay reaction buffer and were then lysed by sonication using a Sonifier 450 (Branson). Cholesterol levels in the embryo lysate were measured with an Amplex Red Cholesterol Assay Kit (Invitrogen) and Flex station II (Bucher Biotec). The total protein concentration of the embryo lysate was measured using a DC protein assay (Bio-Rad Laboratories) and SpectraMax plus (Molecular Devices).

Localization of chimeric proteins

mCherry-RhoCLVL was generated by PCR amplification of mCherry from pmCherry-N3 (a generous gift from S. Walsh) using primers containing sequences coding for the C-terminal 20 amino acid residues of human RhoA. mCherry-RasCVLS was amplified from pME-mCherryCAAX (a generous gift from C.-B. Chien, University of Utah, UT, USA). The PCR products were sub-cloned into pcGlobin2 (Ro et al., 2004) and mRNA was synthesized using the mMESSAGE mMACHINE kit (Ambion). Zebrafish embryos were injected with 250pg of mCherry-RhoCLVL and mCherry-RasCVLS mRNA at the one-cell stage, and raised with or without the presence of 10 μM aplexone at 25°C and fixed at 80% epiboly. Cellular localizations of the mCherry chimeras were analyzed using confocal microscopy.

Cell culture and wound healing assays

HUVECs and HUAECs were purchased from VEC Technologies. Cells were cultured on 0.1% gelatin-coated dishes in Medium 199 (Mediatech), supplemented with 15% fetal bovine serum (ATCC), 48 μg/ml Endothelial Cell Growth Supplement (BD Biosciences), 64 μg/ml heparin sulfate (Sigma-Aldrich), 0.9 mM sodium pyruvate (Mediatech), 100 IU/ml penicillin (Mediatech) and 100 μg/ml streptomycin (Mediatech).

For the wound healing assay, cells were cultured in 24-well plates to confluence before being subjected to a 2-hour pre-treatment with either DMSO, aplexone, rockout (Calbiochem) or NSC 23766 (TOCRIS Bioscience). After the pre-treatment, the monolayer of endothelial cells was scratched and the closure of the wound was measured after 8 hours. The images of wounds were taken at 0 and 8 hours after scratching and the area of the wound was measured using Image J. The migration distance (the width of the wound) was calculated by dividing the area by the length of the wound. Cells below passage seven were used in this study.

Western blotting

Total proteins were prepared by lysis of endothelial cells with sample buffer [62.5 mM, Tris-HCl (pH 6.8), 20% glycerol, 2% SDS, 5% β-mercaptoethanol, 0.025% bromophenol blue) and boiling for 5 minutes.

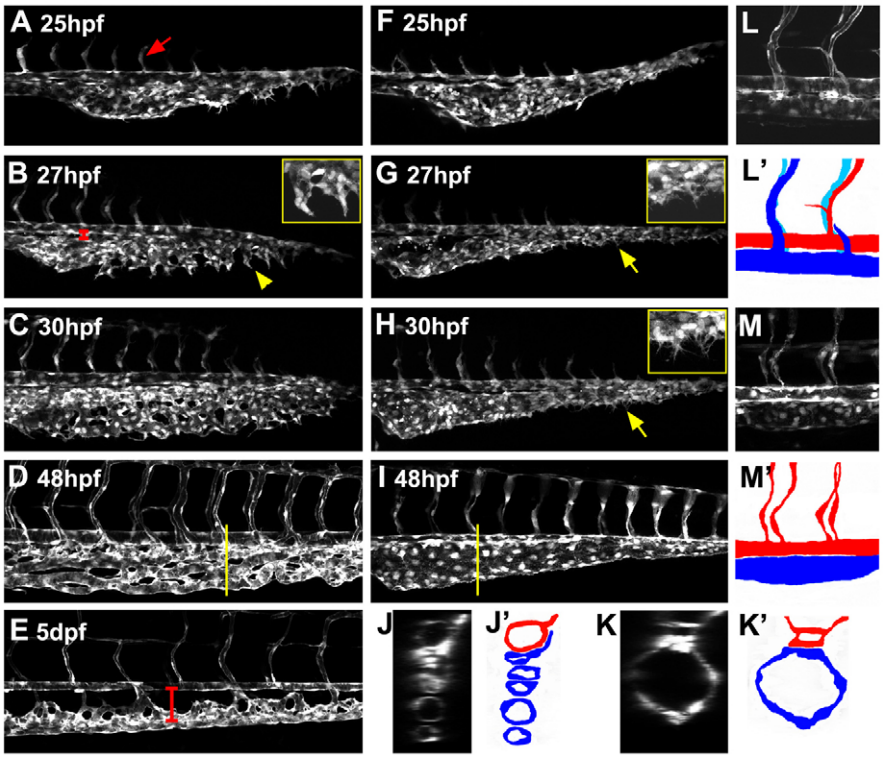

Fig. 1. The development of the zebrafish caudal vein plexus. (**A-I**) Confocal images of caudal vasculature at different developmental stages. (A-E) Untreated control *Tg(kdrl:GFP)* embryos. (F-I) *Tg(kdrl:GFP)* embryos treated with 10 μM aplexone beginning at 10 hpf. The red arrow in A indicates a primary ISV. The yellow arrowhead in B indicates venous angiogenic sprouts. Yellow arrows in G,H indicate filopodia that fail to mature into angiogenic sprouts. Insets in B,G,H are magnified images of the areas indicated by the yellow arrowhead and arrows. Red bars in B and E indicate the distance between the axial artery and vein. (**J**,**K**) Optical cross-sections of blood vessels in control (J) and aplexone-treated (K) embryos at 48 hpf. Yellow bars in D and I indicate the position where the cross-sections were extracted. (**J′**,**K′**) Schematic drawings of the cross-sections in control (J′) and aplexone-treated (K′) embryos. Red represents the dorsal aorta and blue the caudal vein. (**L**,**M**) Confocal images of blood vessels in the trunk of control (L) and aplexone-treated (M) *Tg(kdrl:GFP)* embryos. Images were taken at 48 hpf. (**L′**,**M′**) Schematic drawings of L and M. Red and blue represent the artery and vein, respectively. Horizontal vessels are the dorsal aorta and posterior cardinal vein. Vertical vessels are intersegmental vessels.

The antibodies for RhoA (Santa Cruz Biotechnology) and Rac1 (Millipore) were purchased and the western blots were performed according to the manufacturer's protocols.

Microinjection

tnnt2 MO (8 ng) (Gene Tools) (Sehnert et al., 2002), 3 nl of 4 mM GGTI-2133 (Calbiochem), 3 nl of 5 mM L744,832 (Calbiochem) and 1 nl of 2 M mevalonate (Sigma-Aldrich) were injected into one-to two-cell stage embryos.

RESULTS

Zebrafish caudal vein morphogenesis

At 25 hpf, coinciding with the initiation of blood circulation, the caudal aorta and caudal vein are positioned very closely to each other. Using time-lapse confocal imaging of *Tg(kdrl:GFP)* embryos, we identified a two-stage process involving angiogenesis and vascular remodeling that relocates the caudal vein from its initial position of less than 5 μm ventral to the DA at 27 hpf to a position of 50 μm ventral to the DA after 5 days of development (Fig. 1B,E). Stage I of caudal vein morphogenesis begins at 25 hpf when active angiogenesis is observed in the caudal region. Angiogenic sprouts originating from the caudal aorta migrate dorsally along the boundaries of somites and become ISVs, whereas ECs of the caudal vein send out filopodia at various sites and then migrate ventrally and fuse with neighboring sprouts (Fig. 1A-C). Active sprouting, migration and anastomosis occur in the caudal vein region between 25 hpf and 30 hpf to form the primordial caudal vein plexus (CVP) (see Movie 1 in the supplementary material). Soon after that, sprouting angiogenesis in this region slows down, but the primordial CVP continues to mature and becomes lumenized and serves as a conduit for blood circulation by 36 hpf. Stage II of caudal vein morphogenesis begins at around 48 hpf when active ventral sprouting of ECs of the caudal vein has ceased. During the next few days of development, many endothelial cells of the venous origin in the tail regress restricting flow to the most ventrally positioned vascular channel (Fig. 1E; see Fig. S1 in the supplementary material). Taken together, the morphogenesis of the caudal vein involves sprouting, migration, anastomosis, pruning and regression of ECs originating exclusively from the vein and can therefore serve as an excellent model for venous angiogenesis (Stage I) and remodeling (Stage II) in zebrafish.

Zebrafish chemical screen identifies aplexone as an inhibitor of venous angiogenesis

To understand whether angiogenesis from arterial and venous ECs are under different genetic controls, we screened a collection of small molecules for compounds that preferentially suppress angiogenesis from exclusively one cell type. In this screen, we used the primary ISV sprouts as the readout for arterial-derived angiogenesis, and the CVP and secondary ISV sprouts as indicators of venous-derived angiogenesis. We found one synthetic compound, aplexone, that has a lineage-dependent effect on angiogenesis. The spatial and temporal development of primary ISVs in the trunk is indistinguishable between 2-day-old control and aplexone-treated embryos (Fig. 1L-M′). The formation of the CVP, however, is severely defective in aplexone-treated embryos, resulting in a single-lumen caudal vein (Fig. 1F-I,K; see Movie 2 in the supplementary material). Secondary ISVs are also absent in these embryos (Fig. 1L-M′). In situ hybridization analyses using arterial (*ephrin B2a*) and venous (*flt4* and *ephB4*) markers could not distinguish aplexone-treated embryos from control embryos (Fig. 2), suggesting that treatment with aplexone suppresses venous angiogenesis without affecting arteriovenous differentiation.

We further studied the impact of aplexone on caudal vein angiogenesis at the cellular level. During angiogenesis, ECs send out filopodia followed by the migration of the cell body to form

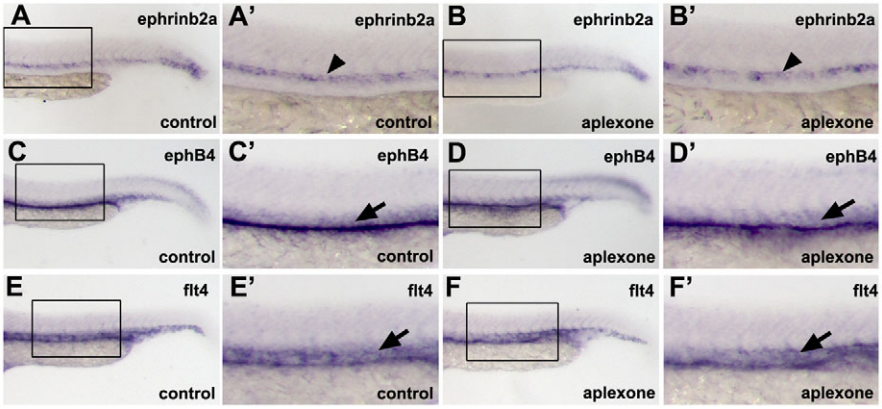

Fig. 2. Aplexone does not affect arterial and venous fate. Untreated control embryos (A,A′,C,C′,E,E′) and embryos treated with 10 μM aplexone beginning at 10 hpf (B,B′,D,D′,F,F′) were fixed at 24 hpf. (**A-F′**) Arterial and venous fates were analyzed by in situ hybridization using *ephrinB2a* (A,A′,B,B′), *ephB4* (C,C′,D,D′) and *flt4* (E,E′,F,F′) probes. Arrowheads indicate the dorsal aorta. Embryos were analyzed at higher magnification in the trunk in A′-F′, with regions of interest indicated by black boxes in A-F. Arrows indicate the posterior cardinal vein.

sprouts. In control embryos, multiple angiogenic sprouts are generated from the caudal vein by 27 hpf (Fig. 1B). Interestingly, although the caudal vein ECs of aplexone-treated embryos formed filopodia, they never matured into angiogenic sprouts (Fig. 1G,H), suggesting a defect in EC migration. We then traced the migration distance of ECs during CVP formation. In vivo time-lapse confocal imaging showed that ECs migrated an average distance of 70 μm between 25 hpf and 30 hpf in control embryos, but only 35 μm in aplexone-treated embryos (Fig. 3A-C; see Movies 3,4 in the supplementary material), demonstrating a strong inhibitory effect of aplexone on venous EC migration.

We next examined the critical time window of application in which aplexone treatment effectively blocks CVP formation. In the first set of experiments, we began the treatment of aplexone at various time points and analyzed CVP formation at 48 hpf. In a second set of experiments, the treatment of aplexone began at 10 hpf and the compound was washed off at various developmental stages. As shown in Fig. 3D, only those embryos exposed to aplexone between 19 and 30 hpf, the time when caudal vein ECs undergo active sprouting, developed a single lumenized caudal vein, demonstrating that aplexone should be present during the active angiogenic phase of caudal vein morphogenesis to block CVP formation.

Hemodynamic flow has a significant impact on vascular remodeling (Lucitti et al., 2007). Aplexone-treated embryos lack blood circulation, raising the issue of whether the effects of aplexone on venous angiogenesis are secondary to the hemodynamic defect. To assess the impact of blood circulation on CVP formation, we used embryos deficient in *tnnt2* or *smoothened* (*smo*), two zebrafish models without circulation (Chen et al., 2001; Sehnert et al., 2002). We found that the formation of angiogenic sprouts is normal and an elaborate primordial CVP is noted in both models by 32 hpf (Fig. 4C,E), indicating that circulation is not required for caudal vein angiogenesis and excluding the notion that the inhibitory effect of aplexone on venous angiogenesis is secondary to a defect in circulation. Interestingly, a single lumen structure is observed in *tnnt2* morphants and *smo* mutant embryos at 48 hpf (Fig. 4D,F), suggesting that the maintenance of the plexus structure of the caudal vein requires proper circulation.

Aplexone modulates the HMG-CoA Reductase pathway

To elucidate the molecular mechanism of action of aplexone, we compared expression profiles of aplexone-treated embryos to DMSO-treated control embryos. Fourteen genes represented on the Affymetrix Zebrafish Genome Array are upregulated by 2-fold or greater in aplexone-treated embryos, including *insig-1* and four genes involved in the HMG-CoA reductase (HMGCR) pathway (see Table S1 in the supplementary material). Quantitative RT-PCR confirmed this finding and further revealed that additional enzymes in the HMGCR pathway that were not represented on the microarray were also upregulated in aplexone-treated embryos (see Table S1 in the supplementary material). Cholesterol is a metabolic product of the HMGCR pathway that negatively regulates the

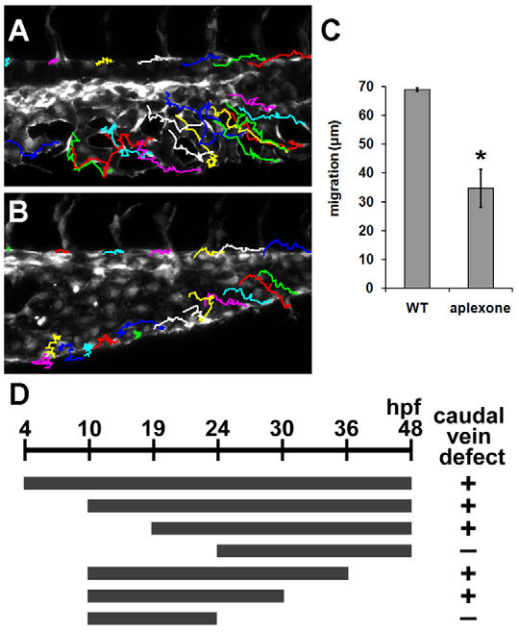

Fig. 3. Aplexone affects the migration of caudal vein endothelial cells. (**A**,**B**) Representative images of the caudal vein of control (A) and 10 μM aplexone-treated (B) embryos at 30 hpf. Images were overlaid with the endothelial cell migration path inferred from time-lapse confocal movies taken from 25 hpf to 30 hpf. The migration of caudal vein endothelial cells was traced using the Manual Tracking feature of ImageJ and the positions of ISV sprouting points were used as references to adjust for the growth of embryos. (**C**) The distance of endothelial cell migration in caudal vein of control and aplexone-treated *Tg(kdrl:GFP)* embryos. Asterisk indicates $P<0.05$. (**D**) The window of application of aplexone. Gray bars represent the developmental stages during which *Tg(kdrl:GFP)* embryos were exposed to 10 μM aplexone and the caudal vein phenotype was analyzed at 48 hpf. + indicates that caudal vein angiogenesis was inhibited. – indicates the formation of normal caudal vein plexus.

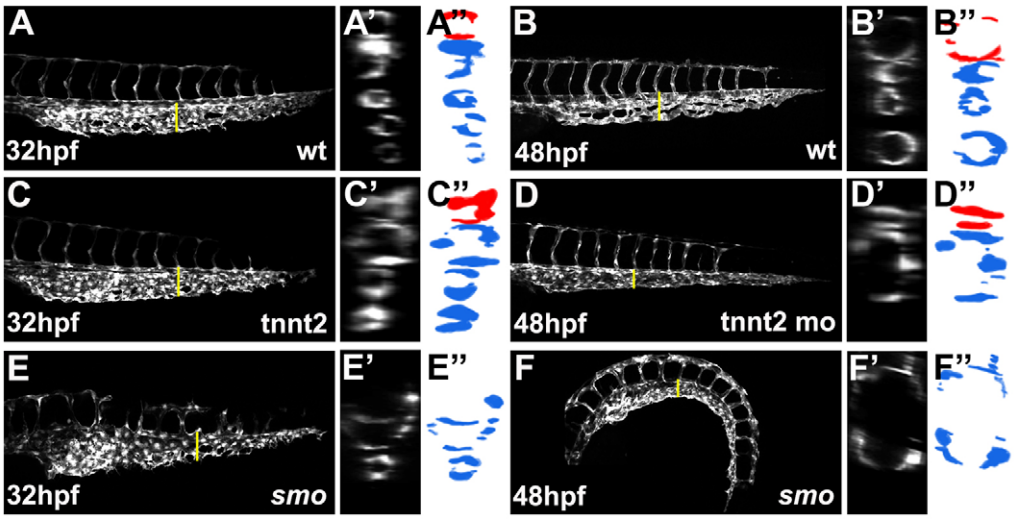

Fig. 4. Blood circulation is not required for sprouting angiogenesis from the caudal vein. (**A**,**B**) Caudal vein plexus in wild-type *Tg(kdrl:GFP)* embryos observed at 32 hpf (A) and 48 hpf (B). (**C-F**) At 32 hpf, the primordial caudal vein plexus was properly formed in *tnnt2* morphant (C) and *smo* mutant (E) embryos, but the plexus structure was not maintained and degenerated into a single-lumen structure at 48 hpf (D,F). (**A′-F′**) Optical cross-sections of blood vessels indicated by yellow lines in A-F. (**A″-F″**) Schematic drawings of images shown in A′-F′. Red and blue represent the artery and vein, respectively.

transcription of *insig-1* and enzymes in the HMGCR pathway (Horton et al., 2002). We found that aplexone reduced embryonic cholesterol levels to a comparable degree to treatment with atorvastatin, a potent inhibitor of HMGCR (Fig. 5B) (Ii and Losordo, 2007). On the contrary, embryos treated with compound AP13, a non-functional aplexone analog, have normal cholesterol levels (Fig. 5B) and normal venous angiogenesis (data not shown), suggesting that, as with atorvastatin, aplexone blocks the HMGCR biochemical pathway.

If aplexone blocks venous angiogenesis via influencing the activity of the HMGCR pathway, one would expect that blocking the same pathway with atorvastatin should impede CVP formation. Indeed, atorvastatin-treated embryos exhibited phenotypes similar to those observed in embryos exposed to aplexone (Fig. 5J). In addition, although embryos treated with suboptimal levels of aplexone (2 μM) or atorvastatin (2 μM) develop a normal CVP, embryos co-treated with suboptimal levels of aplexone and atorvastatin exhibit a single-lumen CVP (Fig. 5F-H), indicating a synergistic effect of atorvastatin and aplexone on venous angiogenesis. Furthermore, injecting mevalonate, a downstream metabolic product of HMGCR, into zebrafish embryos blocks the inhibitory effects of aplexone (Fig. 5M). Together, these findings indicate that aplexone influences venous angiogenesis by modulating the activity of early steps in the HMGCR pathway.

Venous angiogenesis requires protein prenylation

The HMGCR pathway is responsible for the synthesis of isoprene derivatives, which are substrates for protein prenylation, a post-translational modification essential for multiple cellular processes, including cell migration, proliferation and membrane trafficking (Santos and Lehmann, 2004; Thorpe et al., 2004; Bifulco, 2005; D'Amico et al., 2007). Treatment with aplexone severely compromises the migration of ECs, raising the possibility that aplexone inhibits venous angiogenesis by modulating protein prenylation. To evaluate the impact of aplexone on protein prenylation, we generated a chimeric protein with mCherry fused to a CAAX motif from RhoA that was specific for geranylgeranylation, CLVL (Roberts et al., 2008). As expected, the chimeric protein was primarily localized to the plasma membrane in control embryos (Fig. 6E). Upon treatment with aplexone, the chimeric protein was no longer localized predominantly to the membrane and fluorescent signals were present on the membrane as well as in the cytoplasm and nucleus (Fig. 6F). Similar results were observed when we analyzed membrane localization of mCherry proteins fused with a CAAX motif from Ras specific for farnesylation, CVLS (Roberts et al., 2008) (data not shown). These findings demonstrate the inhibitory effect of aplexone on protein prenylation. We then treated zebrafish embryos with GGTI-2133, a geranylgeranyl transferase inhibitor, or L744,832, a farnesyl transferase inhibitor, to evaluate their impacts on venous angiogenesis. We found that although L744,832 does not affect the formation of the CVP (Fig. 6B), embryos injected with GGTI-2133 exhibited CVP phenotypes reminiscent of aplexone treatment (Fig. 6C), suggesting aplexone acts in a Rho-dependent manner. We further analyzed the effects of Rho signaling in CVP formation by blocking the activity of Rho kinases (ROCKs), specific downstream targets of Rho signaling (Riento and Ridley, 2003), using a selective inhibitor, rockout (Yarrow et al., 2005). Treatment with rockout recapitulated the caudal vein phenotype of aplexone treatment (Fig. 6D). Taken together, our findings indicate that farnesylation is not required for CVP formation and that aplexone inhibits CVP formation and EC migration primarily by interfering with protein geranylgeranylation.

Aplexone differentially regulates the migration of human arterial and venous endothelial cells

We next investigated whether aplexone also regulates the migration of human ECs in a wound healing assay using human umbilical vein endothelial cells (HUVECs) and human umbilical artery endothelial cells (HUAECs). Like zebrafish venous ECs, the migration of HUVECs was inhibited by treatment with aplexone and the inhibitory effect became more apparent as the concentration of aplexone increased (Fig. 7A,C). Interestingly, HUAECs exhibited a different response to aplexone. HUAEC migration is unaffected by 5 μM aplexone, a dose sufficient to impede the migration of HUVECs (Fig. 7C). At a concentration of 10 μM, a small, but significant, impediment in HUAEC migration (10%, $P<0.05$) was noted but this inhibitory effect did not appear to have a linear relationship to the dosage of aplexone (Fig. 7C). The differential threshold for response to aplexone between HUVECs and HUAECs indicates that ECs of arterial and venous origins have innate differences in sensitivity to changes in the activity of the HMGCR pathway and suggests that these cells may have differential amounts of proteins subject to

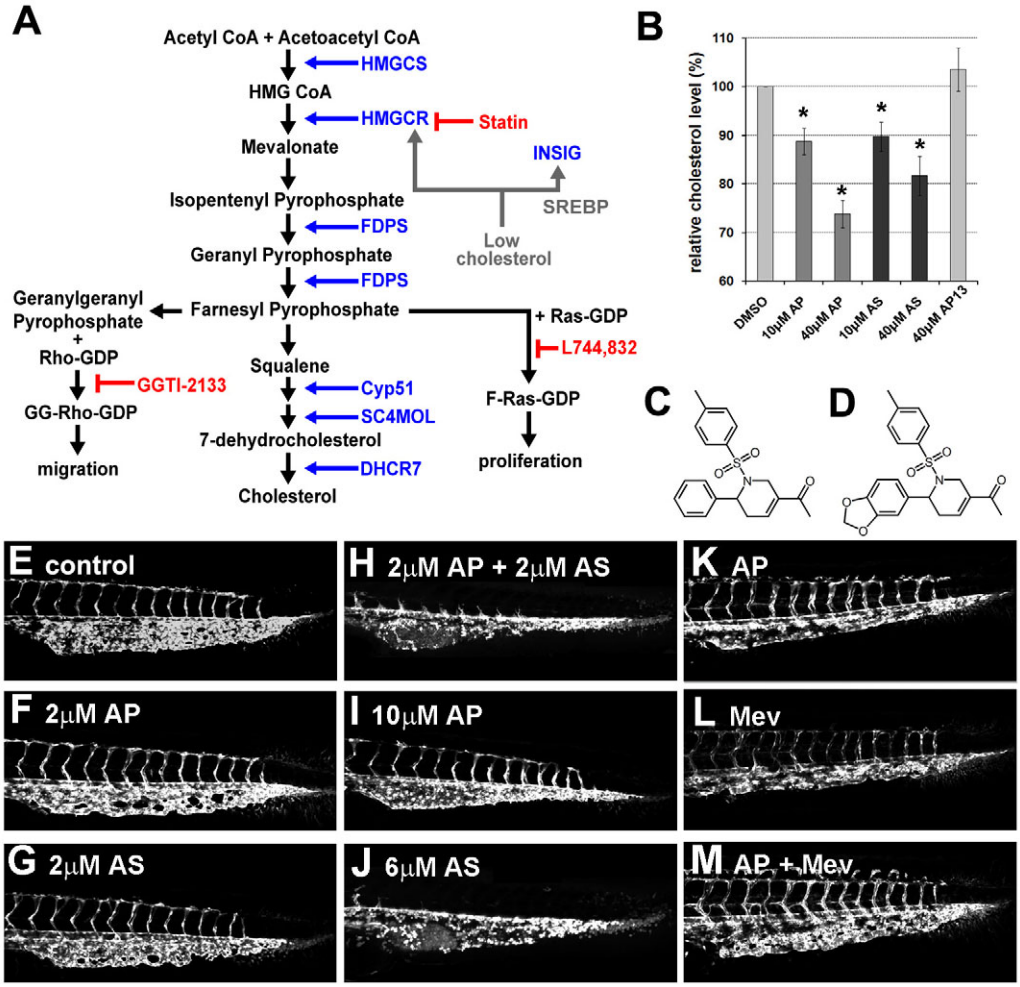

Fig. 5. Aplexone affects the HMGCR pathway. (**A**) Simplified schematic diagram of the HMGCR pathway. Enzymes involved in the pathway are shown in blue. Feedback loop is indicated in gray. Chemical inhibitors of the pathway are indicated in red. HMGCS, 3-hydroxy-3-methylglutaryl-CoA synthase; HMGCR, HMG CoA reductase; FDPS, farnesyl diphosphate synthetase; Cyp51, lanosterol 14 α-demethylase; SC4MOL, sterol-C4-methyl oxidase-like; DHCR7, 7-dehydrocholesterol reductase; INSIG, insulin induced gene 1; SREBP, sterol regulatory element binding proteins. (**B**) Relative cholesterol levels in embryos treated with 0.4% DMSO as a control (DMSO), aplexone (AP, structure shown in **C**), atorvastatin (AS) or a non-functional aplexone analog (AP13, structure shown in **D**). Both aplexone and atorvastatin reduce cholesterol levels significantly (*P<0.05). Data are mean±s.e.m. (**E-J**) Aplexone and atorvastatin have a synergistic effect on caudal vein angiogenesis. Embryos were treated with the chemicals indicated beginning at 10 hpf and caudal vein images were taken at 48 hpf. (**K-M**) Mevalonate reverses the effect of aplexone on caudal vein plexus formation. Caudal vein plexus of embryos treated with 5 μM aplexone beginning at 2 hpf (K), injected with 1 nl of 2 M mevalonate (L) or injected with mevalonate followed by aplexone treatment (M).

geranylgeranylation. Indeed, western analysis showed that HUVECs have about 50% more RhoA and Rac1, two proteins of the Rho family GTPases that require geranylgeranyl modification for their biological functions (Roberts et al., 2008), than HUAECs (Fig. 7E; see Fig. S2A in the supplementary material), demonstrating an arteriovenous difference in the amounts of CAAX-motif-containing proteins. Rho and Rac play pivotal roles in regulating cytoskeletal dynamics and cell migration. We found that blocking the activity of Rho kinase or Rac1 reduces the migration of HUVECs but has limited impact on the migration of HUAECs (Fig. 7D; see Fig. S2B in the supplementary material), demonstrating that venous ECs are more sensitive to changes of Rho or Rac activity than arterial ECs.

Consistently, zebrafish ECs also showed a differential threshold for responding to aplexone treatment depending on their arteriovenous origins. The vascular defects of zebrafish embryos exposed to 10 μM aplexone are restricted to development of the CVP and the secondary sprouts. However, although embryos subjected to the treatment of a high dose of aplexone (30 μM) develop primary sprouts, these primary ISVs are shorter and never reach the dorsal side of the somites (Fig. 8C′), demonstrating that aorta-derived ECs do respond to aplexone, but require higher doses when compared with ECs of venous origin.

In addition to the vascular defects, embryos treated with a higher dosage of aplexone exhibit multiple morphogenic abnormalities. Embryos exposed to a low dosage of aplexone (10 μM) have a relatively normal body shape and, except for a defect in germ cell migration, the morphogenesis of the internal organs is normal (Fig. 8B,E,F). On the contrary, embryos treated with 30 μM aplexone have additional defects in the fusion of the bilaterally positioned cardiac primordia (Fig. 8C,H,I). Although these embryos are shorter than

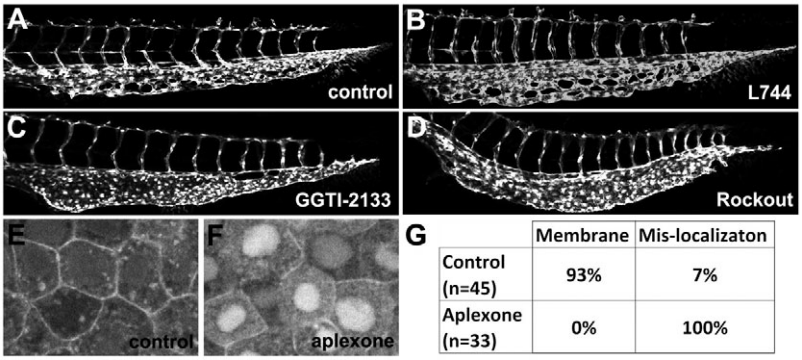

G

	Membrane	Mis-localizaton
Control (n=45)	93%	7%
Aplexone (n=33)	0%	100%

Fig. 6. Aplexone inhibits caudal vein angiogenesis by blocking geranylgeranylation. (**A**) Caudal vein of control *Tg(kdrl:GFP)* embryo at 48 hpf. (**B-D**) Caudal vein of L744,832-injected (B), GGTI-2133-injected (C) or 50 μM rockout-treated (D) *Tg(kdrl:GFP)* embryos analyzed at 48 hpf. (**E**,**F**) Representative confocal images of the localization of mCherry-rhoCAAX fusion proteins in control (E) and aplexone-treated (F) embryos at 80% epiboly. mCherry-rhoCAAX fusion proteins are predominantly localized to the plasma membrane in control embryos but are mislocalized to the nucleus and cytoplasm in aplexone-treated embryos. (**G**) Table quantifying the subcellular localization of mCherry-rhoCAAX in control or aplexone-treated embryos.

control embryos, no evidence suggesting that this is a result of developmental delay was noted. Taken together, our findings demonstrate a crucial role for the HMGCR pathway in regulating the migration of angioblasts, cardiac precursors and primordial germ cells, and a cell type-specific variation in sensitivity to changes in activity of the HMGCR pathway.

DISCUSSION

Endothelial cells assume arterial- or venous-specific molecular characteristics at early developmental stages that instruct later developmental milestones, including lineage-specific anatomical characteristics and physiological functions (Cleaver and Melton, 2003). Disruption of these early molecular programs is detrimental to vascular patterning, as exemplified by the formation of arteriovenous shunts observed in mouse embryos deficient in ephB4 and ephrinB2 (Gerety et al., 1999; Gerety and Anderson, 2002). Studies in zebrafish have shown that endothelial cells of the arterial and venous origins behave differently during early vascular patterning (Isogai et al., 2003; Torres-Vazquez et al., 2003; Jin et al., 2005; Herbert et al., 2009; Hogan et al., 2009; Ellertsdottir et al., 2010; Williams et al., 2010). However, how inherent differences between arterial and venous endothelial cells influence cell type-specific angiogenesis have not been directly investigated. In this report, we characterized the morphogenesis of the caudal vein in the zebrafish and found that the early phase of caudal vein morphogenesis, the formation of the caudal vein plexus (CVP), provides an excellent model for angiogenesis of venous endothelial cells, complementary to the existing model of ISV formation. Using the ISV and CVP as angiogenic models, we identified a novel anti-angiogenic compound, aplexone, in a chemical screen. We found that aplexone effectively inhibits angiogenesis from endothelial cells of venous origin, but has limited effects on arterial angiogenesis both in developing zebrafish embryos and in cultured human endothelial cells, providing evidence that angiogenesis is differentially regulated based on the arterial or venous origin of specific vessels and offering an in vivo system to investigate the underlying molecular and cellular mechanisms.

Several lines of evidence suggest that aplexone regulates venous angiogenesis by modulating the activity of the HMGCR pathway. It is well documented that low cholesterol induces the production of enzymes involved in the HMGCR pathway at the transcriptional level (Horton et al., 2002). The findings that aplexone-treated embryos have reduced levels of cholesterol and elevated transcription of several enzymes of the HMGCR pathway indicate compromised activity of the HMGCR pathway. This, together with the finding that injecting mevalonate, a metabolic product of HMGCR, into zebrafish embryos is sufficient to block the inhibitory effect of aplexone on caudal vein angiogenesis supports the notion that aplexone targets and inhibits the HMGCR pathway. The direct target of aplexone is yet to be identified. However, in light of the rescue effect of mevalonate, it is likely that aplexone acts upstream of mevalonate. Identifying the molecular target of aplexone and evaluating the metabolic processes of aplexone in vivo will provide further understanding on the mechanism of action of this compound.

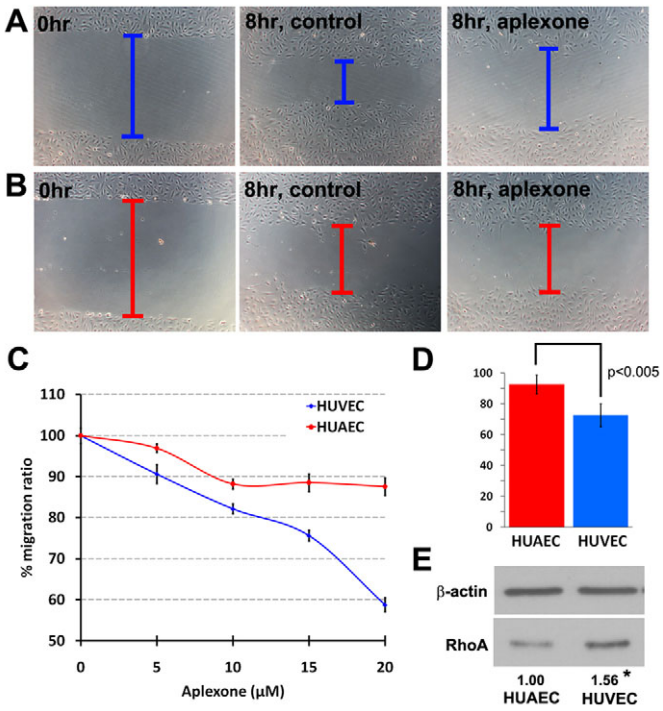

Fig. 7. Aplexone inhibits migration of human endothelial cells. (**A**,**B**) Representative images of wound healing assay. HUVECs (A) and HUAECs (B) at 0 hours and 8 hours after wounds were made. (**C**) The percentage of the migration distance of HUVECs and HUAECs at various aplexone concentrations for 8 hours after wounds were made. Data are mean±s.e.m. (**D**) Graph illustrates the inhibitory effect of 40 μM rockout, a Rho kinase inhibitor, on HUVECs and HUAECs. Data are mean±s.e.m. (**E**) A representative image of western blot for total RhoA in HUAECs and HUVECs. The same blot was probed with anti-β-actin antibody to verify equal loading. The average of the relative amounts of total RhoA in HUAECs and HUVECs collected from four independent experiments is indicated under the western blot (*P<0.05).

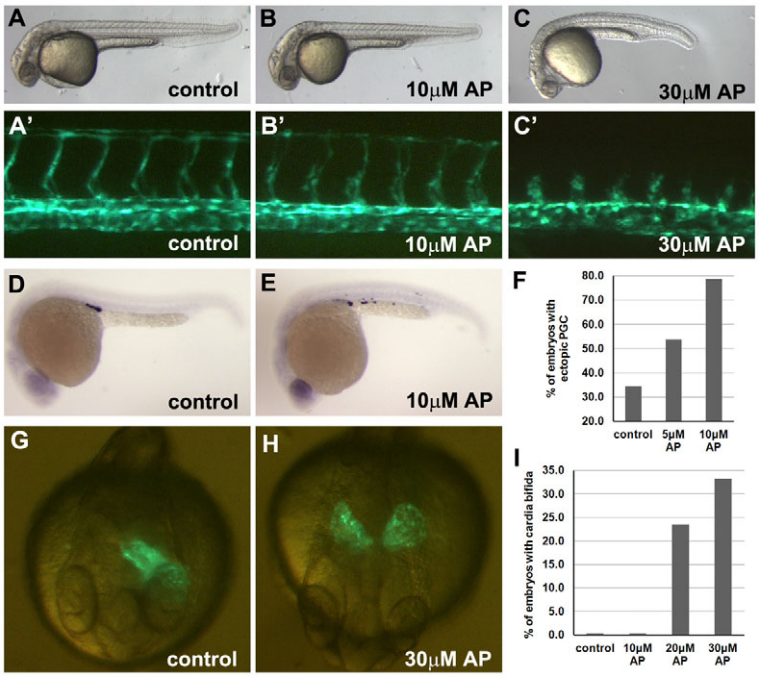

Fig. 8. Aplexone inhibits migration of germ cells, cardiomyocytes and arterial endothelial cells. (**A**,**B**,**C**) Overall phenotype of control and aplexone-treated embryos at 30 hpf. (**A′**,**B′**,**C′**) Vasculature in trunk. Aplexone (10 μM) does not affect the development of primary ISVs but 30 μM aplexone inhibits the growth of primary ISVs. (**D**,**E**) Germ cells in control (D) and aplexone-treated (E) embryos at 24 hpf were detected by in situ hybridization using the *nanos* probe. (**F**) The percentage of embryos with ectopic primordial germ cells in control (n=26), 5 μM (n=13) and 10 μM (n=14) aplexone-treated embryos. (**G**,**H**) Cardiomyocytes migrate to the midline and form a heart tube in *Tg(myl7:GFP)* embryos by 24 hpf (G), but fail to migrate to midline in embryos treated with 30 μM aplexone (H). (**I**) The percentage of embryos with cardia bifida in control (n=16) and 10 μM (n=17), 20 μM (n=17) and 30 μM (n=18) aplexone-treated embryos.

The HMGCR pathway synthesizes cholesterol as well as multiple isoprene derivatives required for the modification of proteins such as Ras and Rho, the localization and function of which depend on C-terminal prenylation (Bifulco, 2005; Roberts et al., 2008). Using chemical inhibitors, we show that blocking protein geranylgeranylation, but not farnesylation, faithfully recapitulates the aplexone-induced venous angiogenesis phenotypes in developing zebrafish embryos and the cell migration defects in human endothelial cells, indicating that aplexone inhibits endothelial cell migration by interfering with the geranylgeranylation branch of the HMGCR pathway. In addition, we noted that different cell types had various sensitivities to the treatment of aplexone. Embryos treated with a low concentration of aplexone have normal morphogenesis with defects restricted to venous angiogenesis and germ cell migration, whereas embryos exposed to a high dose of aplexone have shorter primary ISVs and impaired formation of the primitive heart tube. This finding is consistent with previous genetic observations that the HMGCR pathway regulates germ cell migration and heart tube formation via modulating the production of isoprenoids in *Drosophila* and zebrafish (Santos and Lehmann, 2004; Thorpe et al., 2004; Yi et al., 2006; D'Amico et al., 2007). This finding also demonstrates that venous ECs and germ cells are the two cell types most sensitive to changes in protein prenylation, and illustrates crucial regulatory roles for the HMGCR pathway in controlling cell migration in a wide range of tissues. The different sensitivity with respect to angiogenesis between arterial and venous endothelial cells to the suppression of prenylation in both the zebrafish and cultured human endothelial cells suggests that this differential regulation may be a common feature among species. Furthermore, this innate difference in sensitivities to suppression of the activity of the HMGCR pathway correlates with differential amounts of proteins requiring geranylgeranylation expressed in these cells, suggesting that cells of different origins possess differing thresholds of responsiveness to fluctuations in HMGCR activity. This is in agreement with emerging evidence suggesting that cell type-specific proteomes instruct cellular identities and responses to global cues.

Although our study focused on the geranylgeranyl branch of the HMGCR pathway, cholesterol, another metabolic product of this pathway, may also influence endothelial cell behaviors. As an abundant lipid of the cell membrane, the fluctuation of cholesterol levels could affect endocytosis, membrane fluidity and the stability of microdomains and thereby modulate signaling events. In light of recent reports on the essential role of the internalization of VEGF receptor for its signaling (Sawamiphak et al., 2010; Chen et al., 2009), it would be interesting to evaluate whether the treatment of aplexone affects the endocytosis of VEGF receptor. Alternatively, hedgehog (Hh) regulates a cascade of signaling events involving VEGF, Notch and Eph/ephrin in the early specification of arterial cell fate (Lawson et al., 2001; Lawson et al., 2002). As cholesterol modification is required for the proper spatial restriction of Hh proteins, it is possible that changes in cholesterol levels could impact arteriovenous cell fate determination by modulating Hh signaling. In this study, we used a low concentration of aplexone (10 μM) to facilitate our investigation on the differential cellular behaviors between arterial and venous endothelial cells. Under this condition, we noted a slight reduction of embryonic cholesterol levels (~10%) but did not observe any phenotypic changes characteristic of Hh deficiency nor an alteration of arteriovenous cell fates. Whether the treatment of aplexone at high concentration affects endothelial cell biology in a cholesterol-dependent manner would be another interesting line to investigate.

Our study showed that endothelial cells originating from the caudal vein undergo active sprouting, migration and anastomosis to form a primitive plexus between 25 and 30 hpf, which offers an angiogenesis model for venous endothelial cells. In addition to sprouting angiogenesis, the caudal vein morphogenesis provides opportunity for investigating other aspects of vascular biology. For example, we have noted that sprouting and migration become less active in the caudal vein region after 30 hpf. However, the plexus continues to mature and becomes more elaborate, carrying out strong circulation by 36 hpf. It is likely that cellular events resembling intussusception, a non-sprouting angiogenic process often observed during capillary formation, are involved (Makanya et al., 2009), but the precise cellular mechanism underlying the

maturation of the caudal vein plexus awaits further investigation. Furthermore, many endothelial cells in the caudal vein plexus regress after 2 days of development, which consolidates flow into a single lumen at a much more ventral position. Future studies on caudal vein morphogenesis should provide insights into molecular signals controlling vascular remodeling.

Acknowledgements
We thank A. Langenbacher for critical reading of the manuscript; Horst Geiger for his technical assistance in microarray analysis; S. Castellano, T. A. Dwight and I. P. Andrews for their help with chemical synthesis; members of the Kwon and Chen laboratories for stimulating discussions; and J. Saxe and J. Huang for providing the BioMol library for screening. This work was supported by a Margret E. Early award to J.N.C.; by NIH grants R01HL081700 (to J.N.C.), R01GM071779 and P41GM081282 (to O.K.); by Contract LSHG-CT-2003-503496; by ZF-MODELS project (to R.G. and G.W.O.); and by predoctoral fellowships from the American Heart Association (0815206F) to J.C. and the Training Program of Genetic Mechanisms to K.M. Deposited in PMC for release after 12 months.

Competing interests statement
The authors declare no competing financial interests.

Author contributions
J.C. and K.M. designed and performed experiments, interpreted data and co-wrote the manuscript; H.F., S.K. and Z.W. designed and performed experiments on organic synthesis and interpreted data; G.W.O. and R.G. performed microarray and statistical analyses; O.K. designed organic synthesis experiments, interpreted data and co-wrote the manuscript. J.N.C. designed experiments, interpreted data and wrote the manuscript.

Supplementary material
Supplementary material for this article is available at
http://dev.biologists.org/lookup/suppl/doi:10.1242/dev.054049/-/DC1

References

Bifulco, M. (2005). Role of the isoprenoid pathway in ras transforming activity, cytoskeleton organization, cell proliferation and apoptosis. *Life Sci.* **77**, 1740-1749.
Castellano, S., Fiji, H. D., Kinderman, S. S., Watanabe, M., Leon, P., Tamanoi, F. and Kwon, O. (2007). Small-molecule inhibitors of protein geranylgeranyltransferase type I. *J. Am. Chem. Soc.* **129**, 5843-5845.
Chen, M., Philipp, M., Wang, J., Premont, R. T., Garrison, T. R., Caron, M. G., Lefkowitz, R. J. and Chen, W. (2009). G Protein-coupled receptor kinases phosphorylate LRP6 in the Wnt pathway. *J. Biol. Chem.* **284**, 35040-35048.
Chen, W., Burgess, S. and Hopkins, N. (2001). Analysis of the zebrafish smoothened mutant reveals conserved and divergent functions of hedgehog activity. *Development* **128**, 2385-2396.
Choi, J., Dong, L., Ahn, J., Dao, D., Hammerschmidt, M. and Chen, J. N. (2007). FoxH1 negatively modulates flk1 gene expression and vascular formation in zebrafish. *Dev. Biol.* **304**, 735-744.
Cleaver, O. and Melton, D. A. (2003). Endothelial signaling during development. *Nat. Med.* **9**, 661-668.
D'Amico, L., Scott, I. C., Jungblut, B. and Stainier, D. Y. (2007). A mutation in zebrafish hmgcr1b reveals a role for isoprenoids in vertebrate heart-tube formation. *Curr. Biol.* **17**, 252-259.
Ellertsdottir, E., Lenard, A., Blum, Y., Krudewig, A., Herwig, L., Affolter, M. and Belting, H. G. (2010). Vascular morphogenesis in the zebrafish embryo. *Dev. Biol.* **341**, 56-65.
Gerety, S. S. and Anderson, D. J. (2002). Cardiovascular ephrinB2 function is essential for embryonic angiogenesis. *Development* **129**, 1397-1410.
Gerety, S. S., Wang, H. U., Chen, Z. F. and Anderson, D. J. (1999). Symmetrical mutant phenotypes of the receptor EphB4 and its specific transmembrane ligand ephrin-B2 in cardiovascular development. *Mol. Cell* **4**, 403-414.
Herbert, S. P., Huisken, J., Kim, T. N., Feldman, M. E., Houseman, B. T., Wang, R. A., Shokat, K. M. and Stainier, D. Y. (2009). Arterial-venous segregation by selective cell sprouting: an alternative mode of blood vessel formation. *Science* **326**, 294-298.
Hogan, B. M., Herpers, R., Witte, M., Helotera, H., Alitalo, K., Duckers, H. J. and Schulte-Merker, S. (2009). Vegfc/Flt4 signalling is suppressed by Dll4 in developing zebrafish intersegmental arteries. *Development* **136**, 4001-4009.
Horton, J. D., Goldstein, J. L. and Brown, M. S. (2002). SREBPs: transcriptional mediators of lipid homeostasis. *Cold Spring Harb. Symp. Quant. Biol.* **67**, 491-498.
Huang, C. J., Tu, C. T., Hsiao, C. D., Hsieh, F. J. and Tsai, H. J. (2003). Germ-line transmission of a myocardium-specific GFP transgene reveals critical regulatory elements in the cardiac myosin light chain 2 promoter of zebrafish. *Dev. Dyn.* **228**, 30-40.
Ii, M. and Losordo, D. W. (2007). Statins and the endothelium. *Vascul. Pharmacol.* **46**, 1-9.
Irizarry, R. A., Hobbs, B., Collin, F., Beazer-Barclay, Y. D., Antonellis, K. J., Scherf, U. and Speed, T. P. (2003). Exploration, normalization, and summaries of high density oligonucleotide array probe level data. *Biostatistics* **4**, 249-264.
Isogai, S., Lawson, N. D., Torrealday, S., Horiguchi, M. and Weinstein, B. M. (2003). Angiogenic network formation in the developing vertebrate trunk. *Development* **130**, 5281-5290.
Jin, S. W., Beis, D., Mitchell, T., Chen, J. N. and Stainier, D. Y. (2005). Cellular and molecular analyses of vascular tube and lumen formation in zebrafish. *Development* **132**, 5199-5209.
Kimmel, C. B., Ballard, W. W., Kimmel, S. R., Ullmann, B. and Schilling, T. F. (1995). Stages of embryonic development of the zebrafish. *Dev. Dyn.* **203**, 253-310.
Lawson, N. D., Scheer, N., Pham, V. N., Kim, C. H., Chitnis, A. B., Campos-Ortega, J. A. and Weinstein, B. M. (2001). Notch signaling is required for arterial-venous differentiation during embryonic vascular development. *Development* **128**, 3675-3683.
Lawson, N. D., Vogel, A. M. and Weinstein, B. M. (2002). sonic hedgehog and vascular endothelial growth factor act upstream of the Notch pathway during arterial endothelial differentiation. *Dev. Cell* **3**, 127-136.
Lucitti, J. L., Jones, E. A., Huang, C., Chen, J., Fraser, S. E. and Dickinson, M. E. (2007). Vascular remodeling of the mouse yolk sac requires hemodynamic force. *Development* **134**, 3317-3326.
Makanya, A. N., Hlushchuk, R. and Djonov, V. G. (2009). Intussusceptive angiogenesis and its role in vascular morphogenesis, patterning, and remodeling. *Angiogenesis* **12**, 113-123.
R Development Core Team (2010). *R: A Language and Environment for Statistical Computing*. Vienna, Austria: R Foundation for Statistical Computing.
Riento, K. and Ridley, A. J. (2003). Rocks: multifunctional kinases in cell behaviour. *Nat. Rev. Mol. Cell Biol.* **4**, 446-456.
Ro, H., Soun, K., Kim, E. J. and Rhee, M. (2004). Novel vector systems optimized for injecting in vitro-synthesized mRNA into zebrafish embryos. *Mol. Cells* **17**, 373-376.
Roberts, P. J., Mitin, N., Keller, P. J., Chenette, E. J., Madigan, J. P., Currin, R. O., Cox, A. D., Wilson, O., Kirschmeier, P. and Der, C. J. (2008). Rho Family GTPase modification and dependence on CAAX motif-signaled posttranslational modification. *J. Biol. Chem.* **283**, 25150-25163.
Santos, A. C. and Lehmann, R. (2004). Isoprenoids control germ cell migration downstream of HMGCoA reductase. *Dev. Cell* **6**, 283-293.
Sawamiphak, S., Seidel, S., Essmann, C. L., Wilkinson, G. A., Pitulescu, M. E., Acker, T. and Acker-Palmer, A. (2010). Ephrin-B2 regulates VEGFR2 function in developmental and tumour angiogenesis. *Nature* **465**, 487-491.
Sehnert, A. J., Huq, A., Weinstein, B. M., Walker, C., Fishman, M. and Stainier, D. Y. (2002). Cardiac troponin T is essential in sarcomere assembly and cardiac contractility. *Nat. Genet.* **31**, 106-110.
Smyth, G. K. (2004). Linear models and empirical bayes methods for assessing differential expression in microarray experiments. *Stat. Appl. Genet. Mol. Biol.* **3**, Article3.
Thorpe, J. L., Doitsidou, M., Ho, S. Y., Raz, E. and Farber, S. A. (2004). Germ cell migration in zebrafish is dependent on HMGCoA reductase activity and prenylation. *Dev. Cell* **6**, 295-302.
Torres-Vazquez, J., Kamei, M. and Weinstein, B. M. (2003). Molecular distinction between arteries and veins. *Cell Tissue Res.* **314**, 43-59.
Walsh, D. P. and Chang, Y.-T. (2006). Chemical genetics. *Chem. Rev.* **106**, 2476-2530.
Wang, H. U., Chen, Z. F. and Anderson, D. J. (1998). Molecular distinction and angiogenic interaction between embryonic arteries and veins revealed by ephrin-B2 and its receptor Eph-B4. *Cell* **93**, 741-753.
Westerfield, M. (2000). *The Zebrafish Book*. Eugene, OR: The University of Oregon Press.
Williams, C., Kim, S. H., Ni, T. T., Mitchell, L., Ro, H., Penn, J. S., Baldwin, S. H., Solnica-Krezel, L. and Zhong, T. P. (2010). Hedgehog signaling induces arterial endothelial cell formation by repressing venous cell fate. *Dev. Biol.* **341**, 196-204.
Yarrow, J. C., Totsukawa, G., Charras, G. T. and Mitchison, T. J. (2005). Screening for cell migration inhibitors via automated microscopy reveals a Rho-kinase inhibitor. *Chem. Biol.* **12**, 385-395.
Yi, P., Han, Z., Li, X. and Olson, E. N. (2006). The mevalonate pathway controls heart formation in Drosophila by isoprenylation of Ggamma1. *Science* **313**, 1301-1303.
Zhong, T. P., Childs, S., Leu, J. P. and Fishman, M. C. (2001). Gridlock signalling pathway fashions the first embryonic artery. *Nature* **414**, 216-220.
Zhu, X., Lan, J. and Kwon, O. (2003). An expedient phosphine-catalyzed [4 + 2] annulation: synthesis of highly functionalized tetrahydropyridines. *J. Am. Chem. Soc.* **125**, 4716-4717.
Zon, L. I. and Peterson, R. T. (2005). In vivo drug discovery in the zebrafish. *Nat. Rev. Drug Discov.* **4**, 35-44.

Table S1. Enzymes involved in the HMGCR pathway are upregulated in aplexone-treated embryos

Gene	Microarray	qPCR
Glutathione S-transferase	3.2	
Selenoprotein W	3.1	
Sulfotransferase	3.0	
Cytochrome P450, family 51 (CYP51)	2.8	4.4
Insulin induced gene 1 (INSIG)	2.6	5.1
Fatty acid desaturase 2	2.4	
Glutathione reductase like	2.2	
Glutamate dehydrogenase 1a	2.2	
Krueppel-like factor 11 (TIEG-2)	2.1	
Carbonyl reductase 1-like	2.1	
Insulin-like growth factor binding protein 1	2.1	
3-Hydroxy-3-methylglutaryl-Coenzyme A synthase 1 (HMGCS)	2.0	2.8
Farnesyl diphosphate synthetase (FDPS)	2.0	2.2
Sterol-C4-methyl oxidase-like (SC4MOL)	2.0	5.6
3-Hydroxy-3-methylglutaryl-Coenzyme A reductase (HMGCR)		6.7
7-Dehydrocholesterol reductase (DHCR7)		2.5
Coronin, actin binding protein, 1A	–2.1	
Myosin regulatory light chain interacting protein	–2.1	
Nephrosin	–2.4	
Lymphocyte cytosolic plastin 1	–2.7	
Lysozyme	–2.7	

The genes that up- or downregulated more than twofold in aplexone-treated embryos are listed. Fold changes of the gene in aplexone-treated embryos detected by microarray and quantitative RT-PCR are indicated on the right.

Table S2. Primers used in quantitative PCR and generating chimeric proteins

Gene		Primer sequences
hmgcs1	Forward	5'- TGAAGAGTCGGGCAACACTGATGT-3'
hmgcs1	Reverse	5'-GCAATATCACCAGCAACAACCAGAGC-3'
hmgcr	Forward	5'-GCTTTGGCCAAGTTTGCTCTGAGT-3'
hmgcr	Reverse	5'-TCCACGAGGGCATCAAGAGTGAAA-3'
fdps	Forward	5'-GATCCTGTTCTCAGTGATGCCCTCAA-3'
fdps	Reverse	5'-ACTTCCTCAGTTGGCAGCTCAGAT-3'
cyp51	Forward	5'-TTCAGACGGAGAGATCGAGCACAT-3'
cyp51	Reverse	5'-TCTCGGTATCTTCTCTGCGCTTCTTG-3'
sc4mol	Forward	5'-GGAAGTGCTTCAAGATGCTGCTGT-3'
sc4mol	Reverse	5'-GTGTCCCAGTCATAAGGGATGCTGAA-3'
dhcr7	Forward	5'-TAAGCAGCAGGAGCTGTATGGTTACG-3'
dhcr7	Reverse	5'-GTCTTCAGGTACCAGGCTTCATTCCA-3'
insig1	Forward	5'-AGAGGAAGTGCTGGACACGCTATT-3'
insig1	Reverse	5'-CGCTTGAACTTGTGTGGTTCTCCAAG-3'
gapdh	Forward	5'- TGTGATGGGAGTCAACCAGGACAA-3'
gapdh	Reverse	5'- TTAGCCAGAGGAGCCAAGCAGTTA-3'
cherry-RhoA	Forward	5'-GGATCCACCATGGTGAGCAAGGGCGAG-3'
cherry-RhoA	Reverse	5′-GAATTCTCACAAGACAAGGCACCCAGATT TTTTCTTCCCACGTCTAGCTTGCAGAGCAGCT CTCGTCTTGTACAGCTCGTCCATGCC-3′
cherry-Ras	Forward	5′-ACGTCGGATCCACCATGGTGAGCAAGG-3'
cherry-Ras	Reverse	5′-ACGTCGAATTCAGGAGAGCACACACTTGC-3'